Variable carrier reduction in radio-over-fiber systems for increased modulation efficiency using a Si_3N_4 tunable extinction ratio ring resonator

Andreas Perentos,[1,*] Francisco Cuesta-Soto,[2] Manuel Rodrigo,[2] Antonio Canciamilla,[3] Borja Vidal,[4] Luigi Pierno,[5] Amadeu Griol,[4] N. S. Losilla,[4] Laurent Bellieres,[4] Francisco Lopez-Royo,[4] Andrea Melloni,[3] and Stavros Iezekiel[1]

[1]*Department of Electrical & Computer Engineering, University of Cyprus, Nicosia 1678, Cyprus*
[2]*DAS Photonics, Ciudad Politécnica de la Innovación, Valencia 46022, Spain*
[3]*Dipartimento di Elettronica e Informazione, Politecnico di Milano, Milan 20133, Italy*
[4]*Valencia Nanophotonics Technology Center, Universitat Politècnica de València, Valencia 46022, Spain*
[5]*SELEX Sistemi Integrati S.p.A., Rome 00131, Italy*
[*]*perentos@ucy.ac.cy*

Abstract: Variable optical carrier reduction via the use of a Si_3N_4 ring resonator notch filter with tunable extinction ratio is demonstrated in a 10 GHz radio-over-fiber system for improving the modulation efficiency. The extinction of the filter notch is tuned with micro-heaters, by setting the Mach-Zehnder coupler of the ring. Experimental results showing a modulation depth improvement of up to 20 dB are provided.

OCIS codes: (060.5625) Radio frequency photonics; (060.2360) Fiber optics links and subsystems; (130.7408) Wavelength filtering devices; (230.5750) Resonators.

References and links

1. C. Lim, A. Nirmalathas, M. Bakaul, P. Gamage, Ka-Lun Lee, Yizhuo Yang, D. Novak, and R. Waterhouse, "Fiber-wireless networks and subsystem technologies," J. Lightwave Technol. **28**(4), 390–405 (2010).
2. J. Capmany and D. Novak, "Microwave photonics combines two worlds," Nat. Photonics **1**(6), 319–330 (2007).
3. N. Gomes, M. Morant, A. Alphones, B. Cabon, J. Mitchell, C. Lethien, M. Csörnyei, A. Stöhr, and S. Iezekiel, "Radio-over-fiber transport for the support of wireless broadband services [Invited]," J. Opt. Netw. **8**(2), 156–178 (2009).
4. K. J. Williams and R. D. Esman, "Stimulated Brillouin scattering for improvement of microwave fibre-optic link efficiency," Electron. Lett. **30**(23), 1965–1966 (1994).
5. S. Tonda-Goldstein, D. Dolfi, J.-P. Huignard, G. Charlet, and J. Chazelas, "Stimulated Brillouin scattering for microwave signal modulation depth increase in optical links," Electron. Lett. **36**(11), 944–946 (2000).
6. B. Hraimel, X. Zhang, Y. Pei, K. Wu, T. Liu, T. Xu, and Q. Nie, "Optical single-sideband modulation with tunable optical carrier to sideband ratio in radio over fiber systems," J. Lightwave Technol. **29**(5), 775–781 (2011).
7. M. J. LaGasse, W. Charczenko, M. C. Hamilton, and S. Thaniyavarn, "Optical carrier filtering for high dynamic range fiber optic links," Electron. Lett. **30**(25), 2157–2158 (1994).
8. R. D. Esman and K. J. Williams, "Wideband efficiency improvement of fiber optic systems by carrier subtraction," IEEE Photon. Technol. Lett. **7**(2), 218–220 (1995).
9. M. Attygalle, C. Lim, G. J. Pendock, A. Nirmalathas, and G. Edvell, "Transmission improvement in fiber wireless links using fiber Bragg gratings," IEEE Photon. Technol. Lett. **17**(1), 190–192 (2005).
10. C. Lim, M. Attygalle, A. Nirmalathas, D. Novak, and R. Waterhouse, "Analysis of optical carrier-to-sideband ratio for improving transmission performance in fiber-radio links," IEEE Trans. Microw. Theory Tech. **54**(5), 2181–2187 (2006).
11. H. Toda, T. Yamashita, T. Kuri, and K. Kitayama, "25-GHz channel spacing DWDM multiplexing using an arrayed waveguide grating for 60-GHz band radio-on-fiber systems," in *Proceedings of IEEE Microwave Photonics MWP2003*, (Budapest, Hungary, 2003), 287–290.
12. T. Barwicz, M. A. Popović, M. R. Watts, P. T. Rakich, E. P. Ippen, and H. I. Smith, "Fabrication of add-drop filters based on frequency-matched microring resonators," J. Lightwave Technol. **24**(5), 2207–2218 (2006).
13. C. Ferrari, A. Canciamilla, F. Morichetti, M. Sorel, and A. Melloni, "Penalty-free transmission in a silicon coupled resonator optical waveguide over the full C-band," Opt. Lett. **36**(19), 3948–3950 (2011).

#173539 - $15.00 USD Received 30 Jul 2012; revised 8 Sep 2012; accepted 9 Sep 2012; published 25 Oct 2012

14. I. Gasulla, J. Lloret, J. Sancho, S. Sales, and J. Capmany, "Recent breakthroughs in microwave photonics," IEEE Photon. J. **3**(2), 311–315 (2011).
15. J. Capmany, I. Gasulla, and S. Sales, "Microwave photonics: harnessing slow light," Nat. Photonics **5**(12), 731–733 (2011).
16. T. K. Woodward, A. Agarwal, T. Banwell, P. Toliver, B. J. Luff, D. Feng, P. Dong, D. C. Lee, N.-N. Feng, and M. Asghari, "Systems perspectives on optically-assisted RF signal processing using silicon photonics," in *Proceedings of IEEE Microwave Photonics MWP2011*, (Singapore, Singapore, 2011), 377–380.
17. C. Kopp, S. Bernabé, B. B. Bakir, J. Fedeli, R. Orobtchouk, F. Schrank, H. Porte, L. Zimmermann, and T. Tekin, "Silicon photonic circuits: on-CMOS integration, fiber optical coupling, and packaging," IEEE J. Sel. Top. Quantum Electron. **17**(3), 498–509 (2011).
18. D. Guckenberger, "Microwave photonic applications for silicon photonics," in *Proceedings of Optical Fiber Communication OSA/OFC/NFOEC 2009*, (Los Angeles, CA, USA, 2009), 1–3.
19. L. Xu, C. Li, C. W. Chow, and H. K. Tsang, "Optical mm-wave signal generation by frequency quadrupling using an optical modulator and a silicon microresonator filter," IEEE Photon. Technol. Lett. **21**(4), 209–211 (2009).
20. W. Green, R. Lee, G. Derose, A. Scherer, and A. Yariv, "Hybrid InGaAsP-InP Mach-Zehnder racetrack resonator for thermooptic switching and coupling control," Opt. Express **13**(5), 1651–1659 (2005).
21. C. Li, L. Zhou, and A. W. Poon, "Silicon microring carrier-injection-based modulators/switches with tunable extinction ratios and OR-logic switching by using waveguide cross-coupling," Opt. Express **15**(8), 5069–5076 (2007).
22. C. K. Madsen and J. H. Zhao, *Optical Filter Design and Analysis: A Signal Processing Approach* (Wiley, 1999).
23. R. L. Espinola, M. C. Tsai, J. T. Yardley, and R. M. Osgood, "Fast and low-power thermooptic switch on thin silicon-on-insulator," IEEE Photon. Technol. Lett. **15**(10), 1366–1368 (2003).
24. T. Barwicz, M. Popović, P. Rakich, M. Watts, H. Haus, E. Ippen, and H. Smith, "Microring-resonator-based add-drop filters in SiN: fabrication and analysis," Opt. Express **12**(7), 1437–1442 (2004).

1. Introduction

Radio-over-fiber (RoF) is a very attractive technology for meeting the ever increasing bandwidth demands in cellular communications and radar at a low cost [1–3]. Low cost is possible by transferring electronic complexity and bulky components from the base stations to a central office. Additionally, the exploitation of the millimeter-wave frequency regime has opened the path for wider bandwidths. An important performance parameter of a RoF link is the dynamic range, defined as the ratio between the maximum magnitude of the signal and rms of the noise floor. This is determined directly by the modulation depth; the higher the modulation depth, the higher the link efficiency. However, optical modulators have a limited linear region of operation and hence radio frequency signals have to weakly modulate the optical carrier in order to avoid signal distortions. The higher power of the optical carrier in comparison to the sidebands reduces the dynamic range and it can deleteriously affect the performance of components such as electro-optic modulators and photodiodes by exceeding the damage threshold. One technique for circumventing this issue is based on the reduction of the optical carrier immediately after modulation. This technique is useful in systems where the modulation efficiency is limited and the overall optical power cannot be increased due to the danger of saturating the photodetector. Carrier reduction has so far been implemented via Brillouin scattering [4,5], use of dual-parallel Mach-Zehnder modulators [6] and external optical filtering using silica delay lines [7], Fabry-Perot structures [8], fiber Bragg gratings [9,10] and arrayed waveguide gratings (AWG) [11].

Some of these methods are complex while others are not applicable to certain ranges of frequencies and modulation depths [9]. With the exception of the AWG, none of them has the potential for monolithic integration with other optical and electronic devices such as modulators, multiplexers, photodetectors and RF components. Moreover, most of these solutions can provide only a fixed value of rejection, without the possibility to tailor the carrier reduction in order to dynamically optimize the system performance according to the specific transmission conditions. High index contrast photonic technologies, based on silicon or silicon nitride (Si_3N_4), are emerging as promising platforms for reconfigurable passive circuits [12,13] as well as low cost transceivers, such as those required for future microwave photonics [14–16] and RoF applications [17,18]. Additionally, photonic integrated circuits implemented in Si_3N_4 are being proposed as a robust integrated CMOS technology. This

#173539 - $15.00 USD Received 30 Jul 2012; revised 8 Sep 2012; accepted 9 Sep 2012; published 25 Oct 2012

approach results in a flexible tunable filtering solution in a compact device that can be easily integrated with other functionalities in a single photonic integrated chip. Recent advances in CMOS-compatible solutions [17] allow the high levels of integration required of complex circuits in a single chip where optical signals can be modulated, processed and photodetected. These capabilities mark out this technology as a promising alternative with higher efficiency, stability and flexibility compared to existing solutions. Although carrier suppression using a silicon micro-ring resonator has been reported in [19], this was for a fixed amount of suppression. However, a wavelength selective filter for variable optical carrier reduction realized with these technologies would be of great interest to address current RoF limitations in terms of cost and performance.

In this paper we present the first demonstration of a Si_3N_4 ring resonator notch filter with tunable extinction ratio (RNFTE), able to dynamically reduce the optical carrier and enhance the modulation efficiency, in order to finely optimize the performance of RoF links. Proof-of-concept experiments in a 10 GHz RoF link (suitable for application to X-band radar for example) are presented. This method can be easily applied in the mm-wave frequency regime (e.g. for 60 GHz RoF) since the carrier-sideband separation is wider and notch filters with less stringent bandwidth requirements can be used.

2. Si_3N_4 filter design, fabrication and transmission spectrum

2.1 Filter design

In order to realize a variable reduction of optical carrier in RoF systems, a ring resonator based notch filter with tunable extinction ratio (RNFTE) was designed using the methodology in [20,21]. The scheme of the RNFTE is shown in Fig. 1(a).

The coupling (K_r) between the ring (RR) and the bus waveguide is provided here by a Mach-Zehnder (MZ) interferometer, rather than by a standard directional coupler, and can therefore be expressed as [22]:

$$K_r = \cos^2\left(\frac{\Delta\varphi}{2}\right)\sin^2\left(2\kappa L_c\right) \tag{1}$$

where $\Delta\varphi$ is the phase imbalance between the arms of the MZ, while κ and L_c are the coupling coefficient and the coupling length of the directional couplers of the MZ. In this way, the optical power injected into the ring can be varied by changing the phase imbalance $\Delta\varphi$ of the MZ. This allows the coupling coefficient of the ring K_r and thus the extinction ratio ER of the filter (which depends on the ratio between the coupling coefficient and the roundtrip loss in the ring) to be tailored easily. The directional couplers of the MZ are designed to provide 3-dB coupling (i.e. $\kappa L_c = \pi/4$), thus setting the second term of the product in Eq. (1) to unity and therefore guaranteeing the maximum tunability of K_r, from 0 to 1. This means that, irrespective of propagation losses and of their variation due to fabrication tolerances, it is always possible to finely match the critical coupling condition of the filter that provides infinite ER. Moreover, this architecture is also robust to fabrication inaccuracies in the MZ's couplers: even a significant error in κL_c (up to 40%) does not significantly affect the functionality of the device. Although the tunability range of K_r is reduced, the critical coupling condition can be matched for a wide range of propagation losses values (1 dB/cm – 10 dB/cm) and hence the minimum ER of the filter can be achieved.

In this work the MZ is made tunable by exploiting the thermo-optic effect, through a metallic micro-heater (H_1) placed on one of its arms [23]: when an electric current I_{H1} is applied, the temperature of both the metal strip and the underlying waveguide changes. The thermo-optic effect therefore comes into place, by inducing a local change of the optical properties of the waveguide, i.e. of its effective index n_{eff}. A second micro-heater (H_2) is placed on the waveguide of the ring, with a twofold objective: to tune the central wavelength

#173539 - $15.00 USD Received 30 Jul 2012; revised 8 Sep 2012; accepted 9 Sep 2012; published 25 Oct 2012

λ_0 of the filter, by red-shifting the resonance of the ring; and to compensate the slight red-shift induced by the heating of the MZ.

The RNFTE circuit was realized with high index contrast channel waveguides whose cross section is depicted in Fig. 1(b). The Si_3N_4 core dimensions of 300 nm height and 1100 nm width allow single-mode propagation and optimize the TE-polarized mode response, as shown by numerical simulations based on film mode matching method and verified by experimental results. A minimum bending radius of 100 μm is used in the circuit to assure negligible bending losses. The length L_r of the ring resonator was designed to provide a free spectral range (FSR) of 60 GHz and a 3-dB bandwidth not exceeding 18 GHz close to the critical coupling condition. An upper cladding thickness of 1.5 μm guarantees the optimum trade-off between high thermo-optical efficiency of the heaters and low leakage of the optical mode into the metal strips, as verified by numerical simulations. The titanium heaters were designed to have a width of 4 μm and a length L_h = 700 μm, resulting in a resistance of 4.5 kΩ. Experimental characterization shows that, for these actuators, an applied current of only I_H = 4 mA produces a phase shift of 2π, allowing the complete tuning of both K_r (from 1 to 0) and of λ_0 (over a whole FSR).

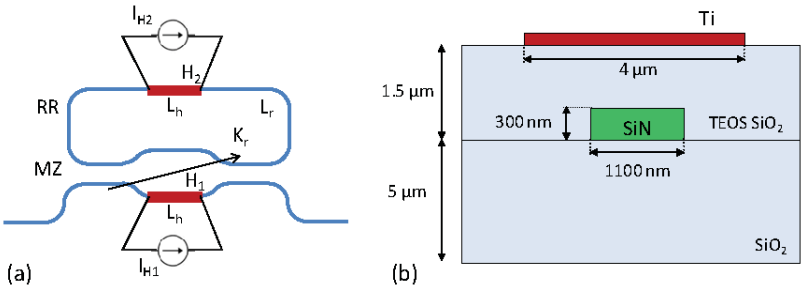

Fig. 1. (a) Scheme of the RNFTE: optical circuit (blue lines), heaters (red lines) and driving electric circuit (black lines); (b) cross section of the SiN waveguide with Ti thermo-optical actuators.

2.2 Filter fabrication

The RNFTE was fabricated using the Si_3N_4 material platform. Commercial substrates were employed with a 300 nm Si_3N_4 top layer deposited by low pressure chemical vapor deposition (LPCVD) on a 5 μm thick SiO_2 bottom cladding layer grown on a 4-inch silicon wafer. The wafer was cleaned with an oxygen plasma and then a hydrogen plasma treatment was applied to enhance photoresist adhesion to the Si_3N_4 surface. The waveguiding structures were patterned on PMMA resist by electron beam lithography employing a Raith150 system operating at 10 keV with an aperture of 30 microns. After resist exposure and development, Cr was evaporated in order to obtain a hardmask by means of the lift-off process with high-pressure NMP as solvent. An optimized etch process in a reactive-ion-etching ICP tool (STS) ensured good and consistent etch profiles. The final dimensions of waveguide and ring resonator were in good agreement with the designs (Fig. 2(a)). After hardmask removal, an upper-cladding layer of 1.5 μm of SiO_2 was deposited over the photonic structures by a TEOS-based PECVD process in an Applied Materials P5000 cluster tool. The micro-heaters pattern was then realized on PMMA aligned to the underlying waveguides and Ti was deposited followed by lift-off. The electrical contacts were subsequently defined with Au by the same method (over a thin Cr adhesion layer), allowing for an overlap section with the Ti micro-heaters. All metals were deposited by physical vapor deposition (PVD) in an e-beam evaporator tool (Pfeiffer Classic 500). Figure 2(b) shows an optical image of the fabricated micro-heater devices.

#173539 - $15.00 USD Received 30 Jul 2012; revised 8 Sep 2012; accepted 9 Sep 2012; published 25 Oct 2012

The flexibility of e-beam lithography allowed us to optimize the design and the fabrication process [24]. The use of e-beam permits the rapid implementation of dose tests to optimize the exposure of every critical element (such as waveguides, couplers and heaters) forming the design pattern, thus leading to a final and complete optimized exposing file. Furthermore, the overall fabrication process in Si_3N_4 technology, including exposure, lift-off processes and reactive ion etching, can be tested and optimized quickly by using e-beam lithography. Similar devices were later fabricated by conventional optical lithography by precise alignment of three mask levels (photonic structures, micro-heaters and electrical pads) using a mask aligner (EVG 620) illuminating with an Hg UV Lamp at 365 nm (i-line).

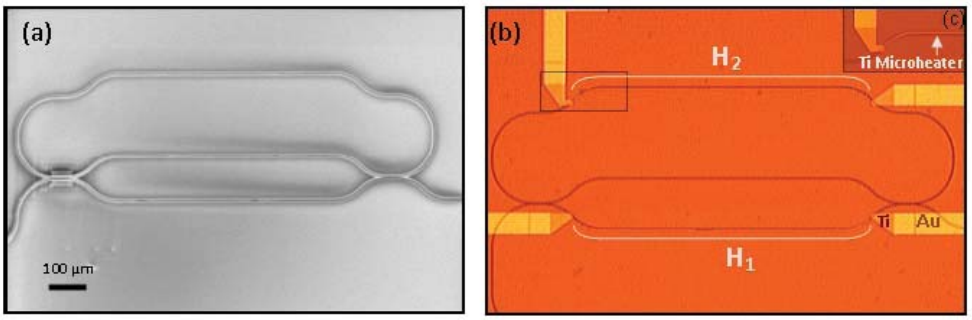

Fig. 2. (a) SEM image of the fabricated RNFTE. (b) optical image of the device with micro-heaters and electrical pad structures. (c) inset (top right of (b)) showing a magnified view of the marked rectangular area in image (b).

2.3 Transmission spectrum measurement

The transmission spectrum of the RNFTE was measured for TE polarization using butt-coupling with lensed fibers. The extinction was continuously varied by changing the current I_{H1} in the heaters. As an example, the optical transmission spectra around the resonance at 1550.39 nm are reported in Fig. 3 for different current values, showing that the ER of the filter can be varied from 5.5 dB to more than 23 dB, by increasing the current I_{H1} by only 1.1 mA and hence the electrical power dissipated in the heater H_1 by 36 mW. The resonant wavelength experiences a slight drift with the change in I_{H1}; this may be easily counteracted by varying the current I_{H2} applied to the heater H_2, in order to center the filter always at the desired wavelength. The compensation was not applied in Fig. 3. An insertion loss of about 19 dB, due to a non optimized fiber-to-waveguide coupling, was achieved. The 3-dB bandwidth of the 23 dB extinction ratio notch was approximately 17 GHz. These parameters are suitable for RoF carrier reduction at 10 GHz and higher frequencies since this value of 3-dB bandwidth will not distort the RF sidebands and the maximum achieved extinction ratio required for carrier reduction is more than adequate.

#173539 - $15.00 USD Received 30 Jul 2012; revised 8 Sep 2012; accepted 9 Sep 2012; published 25 Oct 2012

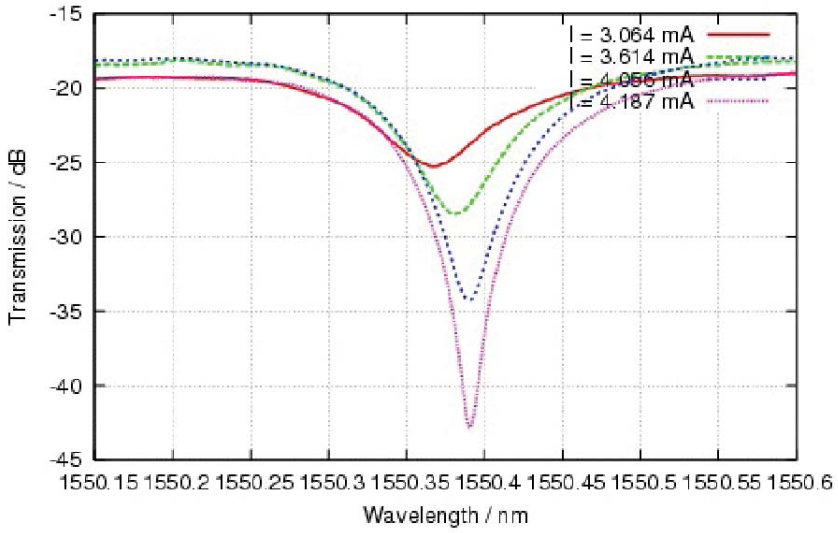

Fig. 3. Ring resonator notch filter with tunable extinction ratio (RNFTE).

3. Application of the Si_3N_4 RNFTE in a 10 GHz RoF system for modulation depth enhancement

The RoF system shown in Fig. 4 was used to evaluate the potential for optical carrier reduction (and hence modulation efficiency enhancement) with the fabricated RNFTE. The tunable laser source (TLS), set at a power of 10 dBm, drove a Mach-Zehnder modulator (MZM) biased at quadrature and the optical carrier was modulated by a 10 GHz RF signal with an RF power of 0 dBm. This produced a double-sideband signal. An erbium doped fiber amplifier (EDFA) was used after the MZM to boost the signal power before entering the RNFTE. An optical bandpass filter (OBPF) was used to reduce the spontaneous emission noise from the EDFA. The RNFTE was inserted in the system along with a polarization controller (PC) in order to select the polarization state of light coupled to the filter. In this experiment, TE polarization was selected for maximum transmission. The RNFTE was used to reduce the optical carrier, having prior set the wavelength at 1550.39 nm in order to be aligned with the filter resonance. In a practical system, the optical carrier would be fixed in wavelength, and the central wavelength of the notch filter would be tuned via I_{H2} in order to align with the carrier. The extinction of the filter notch was tuned by varying the current in the heater H_1. For comparison purposes between the different measurements it is required to fix a constant power at the input of the photodiode (PD). In order to keep the total optical power at the input of the PD constant, as the optical carrier power level would change each time, another EDFA was used at the RNFTE output along with another OBPF. For all current values, the incident power to the PD was kept constant at 0 dBm. It should be mentioned that the presence of two EDFAs is due to the experimental conditions. On one side, an EDFA was needed to compensate the excess losses of the RNFTE. Simple butt coupling was employed and therefore no optimization of power coupling was addressed. Therefore amplification before the filtering is required in order to compensate for the low coupling efficiency. This issue can be solved by using existing coupling solutions, such as grating couplers and inverted tapers, which can improve the coupling efficiency by 5 to 10 dB per port of the device. On the other side, a second EDFA was included to evaluate the response of the system at a constant average power at the photodetector. This helps in the comparison of measurements with different carrier reduction levels. In a real application scenario we may find two different cases. In the first, a high power laser source is employed and the second

#173539 - $15.00 USD Received 30 Jul 2012; revised 8 Sep 2012; accepted 9 Sep 2012; published 25 Oct 2012

EDFA is not needed. In this case the power of the carrier is reduced to prevent damaging the photodetector. In the second case, a power limited link requires amplification anyway and, in order to achieve higher dynamic range, the modulation efficiency needs to be improved as reported in [8].

The optical spectrum was measured with an optical spectrum analyzer (OSA) and the electrical spectrum with an electrical spectrum analyzer (ESA). The aim was to find the current setting of heater H_1 that resulted in the best achievable carrier reduction (i.e. maximum photo-converted RF power). Optimum carrier reduction is achieved when the power level of the carrier aligns with the level of the sidebands. When the power level of the carrier drops below the power level of the sidebands, the photo-converted RF power will decrease again [10]. As the extinction in the filter notch approaches the maximum point, an improvement in the carrier-to-sideband-ratio (CSR) is observed, thus increasing the modulation depth. At the lowest absolute CSR, maximum fundamental RF power is obtained.

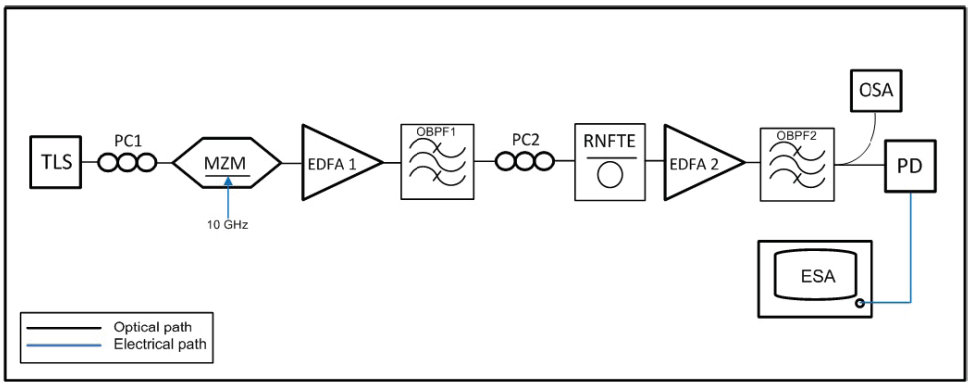

TLS: Tuneable Laser Source	PC: Polarization Controller	MZM: Mach-Zehnder Modulator
EDFA: Erbium Doped Fibre Amplifier	OBPF: Optical Band-Pass Filter	RNFTE: Ring resonator Notch Filter with Tunable Extinction
OSA: Optical Spectrum Analyzer	PD: Photodiode	ESA: Electrical Spectrum Analyzer

Fig. 4. Test bed to evaluate the suitability of the RNFTE for carrier reduction and modulation efficiency enhancement for 10 GHz RoF.

The optical spectra of the modulated signals were initially measured for the values of currents I_{H1} that were used to obtain the transmission spectra in Fig. 3, and the resulting plots are shown in Fig. 5. These show that as the current I_{H1} is increased from 3.064 mA to 4.187 mA, the carrier encounters increasing attenuation relative to the sidebands as a result of the notch in the RNTFE becoming deeper and narrower.

Measurements of the modulated optical spectra were then taken for a larger range of current values I_{H1}, starting with 2.813 mA (for which there is minimal ER in the RNTFE transmission spectrum) up to 5.235 mA (where again there is a minimal resonance in the transmission spectrum). Figure 6 shows the corresponding variation of optical CSR that, for an optical carrier tuned at 1550.39 nm, is reduced by 19.4 dB, ranging from 24.2 dB down to 4.84 dB. The minimum value of CSR is achieved for I_{H1} = 4.187 mA. This is in optimum agreement with the transmission spectra shown in Fig. 3.

#173539 - $15.00 USD Received 30 Jul 2012; revised 8 Sep 2012; accepted 9 Sep 2012; published 25 Oct 2012

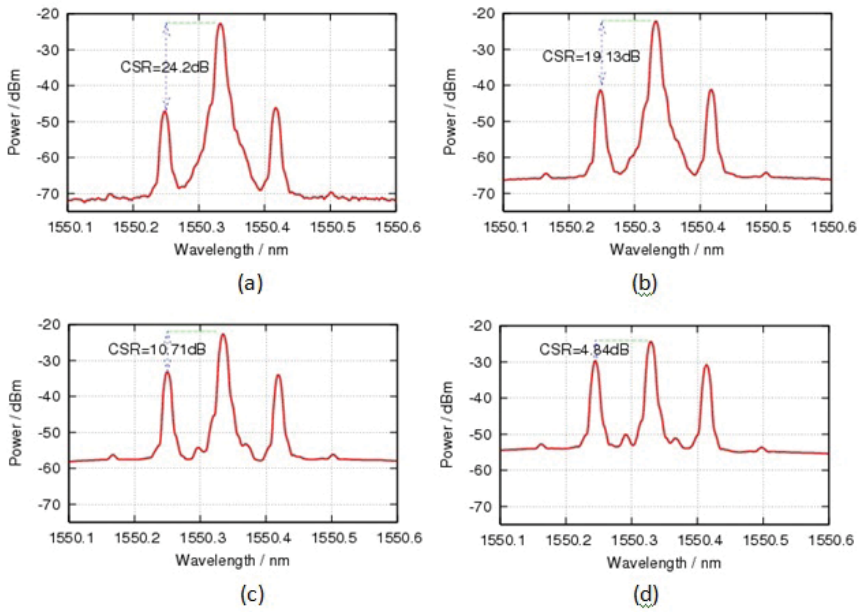

Fig. 5. Optical spectra of the carrier reduced modulated 10 GHz for (a) I = 3.064 mA and CSR = 24.2 dB, (b) I = 3.614 mA and CSR = 19.13 dB, (c) I = 4.056 mA and CSR = 10.71 dB and (d) I = 4.187 mA and CSR = 4.84 dB.

To validate the improvement in the modulation efficiency, the photo-converted signal was analyzed on an ESA. The variation of the fundamental RF power with current I_{H1} is shown in Fig. 7. For a current variation from 2.813 mA to 4.187 mA, the RF power at 10 GHz increases from −59.6 dBm to −39 dBm, which is the maximum point and corresponds to the optimum CSR of 4.84 dB, thus validating the prediction. However, when the current is slightly increased from 4.187 mA to 4.393 mA, a sharp drop in the RF power is experienced going down to −60 dBm before it increases again and 'saturates' at −53 dBm for currents over 4.675 mA. This is due to the heater H_2 not being in use. Hence when I_{H1} is increased, the position of the notch is shifted with respect to the optical carrier, approaching the wavelength of the signal sideband. For values of I_{H1} higher than 4.2 mA, the filter detuning produces intensity and phase distortion of the sideband, resulting in a strong reduction of the measured RF power.

#173539 - $15.00 USD Received 30 Jul 2012; revised 8 Sep 2012; accepted 9 Sep 2012; published 25 Oct 2012

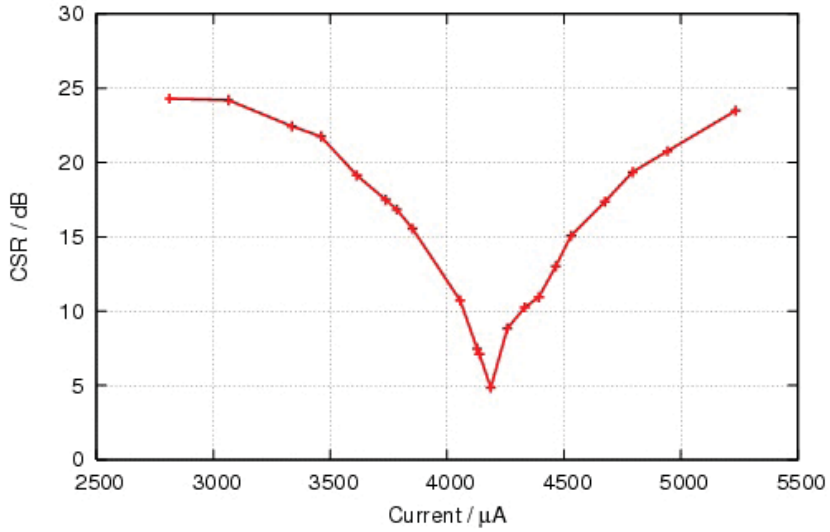

Fig. 6. Optical carrier-to-sideband (CSR) vs current applied to the heaters of the ring resonator.

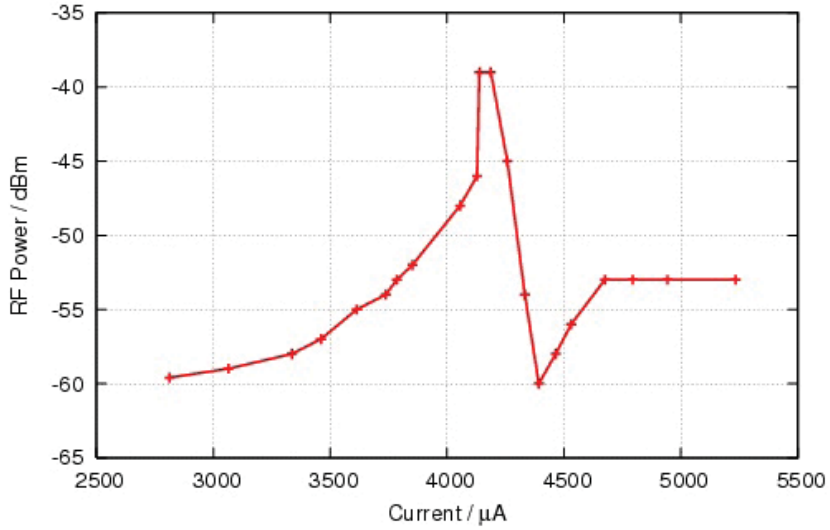

Fig. 7. Measured 10 GHz RF power vs current applied to the heaters of the ring resonator.

To examine the radio frequency operating range of the RNFTE in the system, a microwave vector network analyzer was employed to measure the magnitude and phase response. Using the same system parameters, the RF frequency of the modulator was swept from 100 MHz to 22 GHz at a current of 4.187 mA (Fig. 5(d)) to operate at maximum extinction and hence maximum RF power. The results for the magnitude and phase can be seen in Figs. 8 and 9 respectively. From Fig. 8, it can be concluded that the RNFTE can be used for RF frequencies greater than 5 GHz (the limitation being due to the relatively large 3-dB bandwidth of the RNFTE at maximum extinction point). The measured phase of the system has been processed for unwrapping and it is shown in Fig. 9. It can be observed that the phase is quite linear with no distortion at the frequencies of the sidebands. The inset of Fig. 9 shows the expected 2π phase shift in the resonance frequency due to the ring resonator.

#173539 - $15.00 USD Received 30 Jul 2012; revised 8 Sep 2012; accepted 9 Sep 2012; published 25 Oct 2012

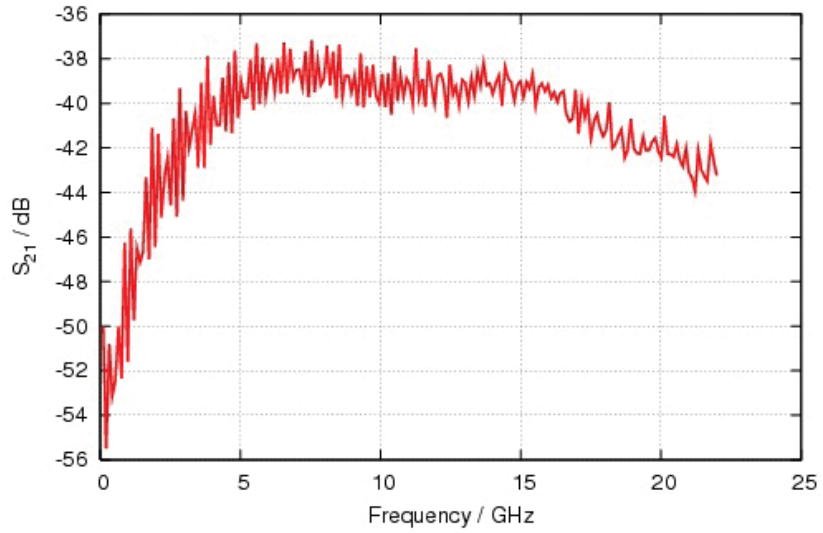

Fig. 8. Measured magnitude transmission response for a frequency sweep 100 MHz-22 GHz.

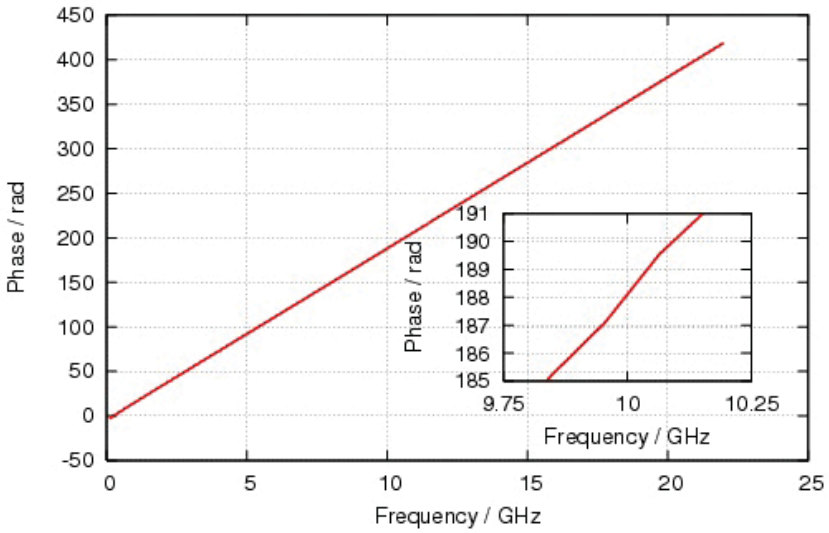

Fig. 9. Measured unwrapped phase response for a frequency sweep 100 MHz-22 GHz.

4. Conclusions

We have demonstrated the use of a Si_3N_4 ring resonator notch filter with tunable extinction (RNFTE) to dynamically and continuously reduce the optical carrier for a 10 GHz RoF system application and hence improve the modulation efficiency of optoelectronic links. The proposed technique allows the control of the modulation depth by varying the extinction level of the RNFTE through thermo-optical actuators. A carrier suppression up to more than 23 dB was demonstrated and a best CSR value of 4.84 dB, corresponding to a maximum RF power of –39 dBm, was achieved for 10 GHz RoF signals. The fabricated RNFTE displays a linear phase response for a frequency range of 100 MHz-22 GHz and is applicable in RoF systems for frequencies over 5 GHz.

#173539 - $15.00 USD Received 30 Jul 2012; revised 8 Sep 2012; accepted 9 Sep 2012; published 25 Oct 2012

This method is simple and offers future scope for monolithic integration on silicon chips with other optical devices and RF components as part of a photonic integrated circuit for RoF and other microwave photonic applications such as antenna remoting. Although the experimental test set-up employs EDFAs, the use of these can be avoided in a practical application. This may be achieved, for example, by improving the coupling efficiency between the RNFTE and its input and output fibers.

Acknowledgments

This work was supported by the NANOCAP project A-1084-RT-GC that is coordinated by the European Defence Agency (EDA) and funded by 11 contributing Members (Cyprus, France, Germany, Greece, Hungary, Italy, Norway, Poland, Slovakia, Slovenia and Spain) in the framework of the Joint Investment Programme on Innovative Concepts and Emerging Technologies (JIP-ICET).

#173539 - $15.00 USD Received 30 Jul 2012; revised 8 Sep 2012; accepted 9 Sep 2012; published 25 Oct 2012